

# MACE — Mach cones in heavy ion collisions

Björn Bäuchle,<sup>1,\*</sup> Laszlo Csernai,<sup>2,3</sup> and Horst Stöcker<sup>1,4,5</sup>

<sup>1</sup>*Institut für Theoretische Physik, Johann Wolfgang Goethe-Universität,  
Max-von-Laue-Str. 1, D-60438 Frankfurt am Main, Germany*

<sup>2</sup>*Section for Theoretical Physics, Departement of Physics,  
University of Bergen, Allégaten 55, 5007 Bergen, Norway*

<sup>3</sup>*KFKI Research Institute for Particle and Nuclear Physics, P.O. Box 49, 1525 Budapest, Hungary*

<sup>4</sup>*Frankfurt Institute for Advanced Studies, Johann Wolfgang Goethe-Universität,  
Max-von-Laue-Str. 1, D-60438 Frankfurt am Main, Germany*

<sup>5</sup>*Gesellschaft für Schwerionenforschung (GSI), D-64220 Darmstadt, Germany*  
(Dated: February 2, 2008)

We study the propagation of sound-like perturbations created by a jet moving with supersonic velocity through the quark-gluon-plasma created in heavy-ion reactions within the model MACE (Mach Cone Evolution). Predictions for heavy-ion reactions at RHIC energies (Au+Au-collisions) and for Pb+Pb reactions at the LHC ( $\sqrt{s} = 5.5A$  TeV) are presented and potential observations by the STAR, PHENIX and ALICE experiments are discussed.

PACS numbers: 24.10.Nz, 25.75.Gz, 25.75.-q

Keywords: Mach cones, collective phenomena, hydrodynamics

## I. INTRODUCTION

First experimental data at the Relativistic Heavy Ion Collider (RHIC) have shown the disappearance of backward correlations in hard processes at central Au+Au-Collisions for high- $p_{\perp}$ -particles [1, 2]. Correlation data with lower  $p_{\perp}$ -threshold for associated particles show a broader peak or even a double-peaked structure in the backward region [3, 4, 5, 6, 7, 8, 9]. Three-particle-correlations [10] seem to support the theory of conical emission [7, 11, 12]. Recently, the observations have been confirmed by preliminary data from the CERES-experiment at the Super Proton Synchrotron (SPS) [13].

Conical structures in heavy ion collisions have been postulated first by Scheid and Greiner already in 1974 [14] and later also by Hofmann, Baumgardt, Stöcker and collaborators in the second half of the 1970s [15, 16, 17, 18, 19, 20, 21, 22, 23, 24, 25]. In that time, strong shock waves in cold nuclear matter were discussed. New interest has been rising in this field in recent years, triggered by the above-named experimental results and new theoretical work from Stöcker and Casalderrey-Solana *et al.* in 2004 [26, 27], and lots of further considerations in the years since [28, 29, 30, 31, 32, 33, 34, 35, 36, 37, 38, 39, 40, 41, 42, 43, 44, 45, 46].

The common idea is that an ultra-relativistic jet which is moving through an extended Quark-Gluon-Plasma will cause some kind of perturbation, maybe sound-like, and thereby lose its energy. Then, it cannot be seen in the experiments anymore. Since the speed of sound is considerably smaller than the speed of light, the perturbations, if indeed sound-like, should interfere constructively along a cone, the so-called Mach cone.

The term “backward hemisphere” is meant relative to one high-energetic trigger-jet. The jet that creates the conical structure is supposed to be opposite to the trigger, i.e. in exact backward direction.

The opening angle  $\beta$  of this cone is in static medium given by

$$\beta = \sin^{-1} \frac{c_s}{v} , \quad (1)$$

where  $c_s$  is the speed of sound in the medium and  $v$  is the velocity of the jet. The cone is supposed to directly emit (or indirectly enhance emission) of particles. Those particles will be found in a circle around the direction of the jet at

$$\alpha = \cos^{-1} \frac{c_s}{v} . \quad (2)$$

In two-particle correlations this scenario will manifest itself as a double-peaked structure in the backward-hemisphere.

The case of non-static medium has been studied in several publications as well for homogeneous, non-static medium as for simplified of full 3+1-dimensional hydrodynamical evolutions of the underlying medium. All of the latter works have described the sound waves and Mach cones within the framework of hydrodynamics and, for that reason, together with the underlying medium.

In the presented work, we develop a model that propagates sound waves through the velocity field as created by applying the hydrodynamical equations and discovers Mach cone structures automatically. Backreaction of jet and sound waves onto the medium is neglected.

## II. HYDRODYNAMICS

A model widely used to describe heavy-ion reactions is fluid- or hydrodynamics. It has been predicted as a

---

\*Electronic address: baeuchle@th.physik.uni-frankfurt.de

key mechanism for the creation of hot and dense matter very early [15, 18]. Using this approach one assumes that the matter described is, at least nearly, in local thermal equilibrium. This is only justified after a short period of time. After that, a locally equilibrated system may be formed. The part of the reaction before equilibration cannot be described by usual (1-fluid-) hydrodynamics.

Therefore, an additional model has to be applied for the creation of the first equilibrated state, the so-called initial state. This can in principle be any kind of non-equilibrium model. The creation of the first equilibrated state can take different times, depending on the mechanism with which it is reached. Times of the order of  $\tau_0 \approx 1$  fm are reasonable.

When the initial state is defined, hydrodynamics start to work. Depending on number and kind of the assumed symmetries in the initial state the fluid development may be solvable analytically or only numerically. Within this stage of the calculations, one has to assume an equation of state (EoS). It must also be chosen if the evolution describes a perfect fluid that is perfectly equilibrated at any point or if small deviations are endorsed. In the latter case, several additional parameters like the heat conductivity, shear- and bulk-viscosity have to be introduced.

In the case of a perfect liquid, there are six equations which have to be solved. Among them are one equation for the conservation of the baryon number density and four for the conservation of energy and momentum:

$$\partial_\mu N^\mu = 0 \quad (3)$$

$$\partial_\mu T^{\mu\nu} = 0 \quad , \quad (4)$$

where the interesting variables are given by

$$N^\mu = \varrho u^\mu \quad (5)$$

$$T^{\mu\nu} = (\varepsilon + P)u^\mu u^\nu - P g^{\mu\nu} \quad . \quad (6)$$

with the local rest frame baryon density  $\varrho$ , the local rest frame energy density  $\varepsilon$ , the pressure  $P$  and the flow velocity  $u^\mu$ .

The sixth equation needed is the EoS which gives a connection between pressure and the densities:

$$P = P(\varepsilon, \varrho) \quad . \quad (7)$$

Within the hydrodynamical framework the propagation of sound waves can be described. The speed of sound  $c_S$  can here be derived from the EoS as

$$c_S^2 = \frac{\partial P}{\partial \varepsilon} \quad . \quad (8)$$

### III. INGREDIENTS

The model developed for this work is independent of the model used for the hydrodynamical evolution. This is because the hydro-evolution is only used as an input for the model, not an inherent part of it. Indeed, any model

that produces a velocity field can be used. However, of course, a different input will alter the results.

Here, we use the Particle in Cell Code (PiC) which bases on the method with the same name developed by Amsden and Harlow in the early 1960s [47, 48] and upgraded to ultra-relativistic energies by Nix and Strottman in the 80s and 90s [49, 50, 51]. The method takes advantage of a combination of Eulerian and Lagrangian solution methods; the pressure is calculated on an Eulerian grid (where the cells are fixed in coordinate space), while all current transfers are calculated in a larger number of Lagrangian cells (where the cells comoving with the fluid).

The initial state for the hydro-evolution is calculated in an effective 1D Yang-Mills coherent field model, where the transverse plane is split up to “streaks” like in the “Firestreak”-model of the 1970s [52, 53]. During the evolution, an ideal gas EoS is used, so that the pressure  $P$  is connected to the energy density  $\varepsilon$  in a very simple way:

$$P = 1/3 \varepsilon \quad , \quad (9)$$

and the speed of sound is given as

$$c_S = 1/\sqrt{3} \approx 0.577 \quad . \quad (10)$$

This corresponds to a first-order approximation onto a Quark-Gluon-Plasma (QGP). The fact that there is no phase transition is justified because the main part of sound wave evolution will take place in this first, hot and dense stage of the reaction.

### IV. MACE

The model “MAch Cones Evolution” (MACE) is built to model the propagation of sound waves through a realistic, relativistic medium. Our approach is to take an existing hydro-evolution and impose a jet and the waves it creates as perturbations. Therefore, no backreaction of jet or sound waves onto the medium can be modelled.

#### A. Jet

Only the away-side-jet (the jet in the backward hemisphere) is considered, since the near-side-jet is not affected by and does not affect the medium.

The jet starts at the first timestep calculated by the hydrodynamical code. This is, depending on the system considered, after few fm after the first collisions.

The jet is created at a given point with a probability that is proportional to the energy-density at that point. The jet’s direction is totally random. The only cut that is applied is the exclusion of all jets that will not end up in the detector. That is, for RHIC-data we take all jets with  $|\eta| < 0.7$  (corresponding to the STAR-TPC), and for LHC-data we cut at  $|\eta| = 0.9$ , which is the acceptance of the ALICE-TPC.

The jet is considered to be high energetic enough not to change its velocity and direction. Calculation of jet quenching is not within the scope of the model. It hence propagates in a straight line with speed of light through the medium. At every timestep, it excites sound waves at its position. These waves are not enhanced in direction of the jet, but are undirected. The direction of the jet will be used for correlation considerations in the end. When out of the medium, the jet does not excite sound waves anymore.

### B. Sound waves

No premature assumptions on the shape of a resulting mach front can be made in an unforeseeable, inhomogeneous and non-statical medium. We will therefore propagate the single elementary waves and identify the wave fronts independent of the propagation. This allows for parts of the elementary waves to become a part of a wave front only after some time and possible deflection. Also, some parts may be swamped away out of the wave front.

So, in order to model the sound waves we create a lot of logical particles, so-called wave markers, at the position of the jet. The word “logical” refers to the fact that we do not assign any physical quantities to these markers yet; they only represent the position and direction of the wave. Random directions will be assigned to the markers, so that after a short propagation in homogeneous medium one elementary wave should indeed be a spherical wave. Such an elementary wave is created at each timestep at the position of the jet. Between the timesteps all “waves”, i.e. all wave markers, are propagated.

The propagation of the wave markers is straightforward: The only assumption made is that they move with the speed of sound relative to the fluid wherever they are. Their direction is adjusted by relativistically adding their initial velocity,  $\vec{v}$ , to the flow-velocity of the underlying medium at the current point,  $\vec{u}$ . This initial velocity  $\vec{v}$  is calculated by multiplying the direction of the wave marker  $\hat{v}$  with the speed of sound:  $\vec{v} = c_s \hat{v}$ .

When a marker crosses the border of a fluid cell, then its current propagation  $\vec{r}' = \vec{r} + \vec{v} \cdot dt$  will be finished with the old velocity, i.e. no deflection happens at the border of two cells. This is justified because the timestep  $dt$  is much smaller than the dimensions of the cells  $dx$ ,  $dy$  and  $dz$ .

If a marker leaves the system, it is deleted. No particle emission at this point is assumed, and the wave is also not reflected. Fig. 1 shows the position of markers after 10 timesteps of an exemplified propagation (here, the data for a peripheral collision at RHIC have been applied).

It should be noted that, by conserving the number of wave markers per elementary wave, their “amplitude” will decrease with the  $1/r^2$ -behaviour expected for spherical waves.

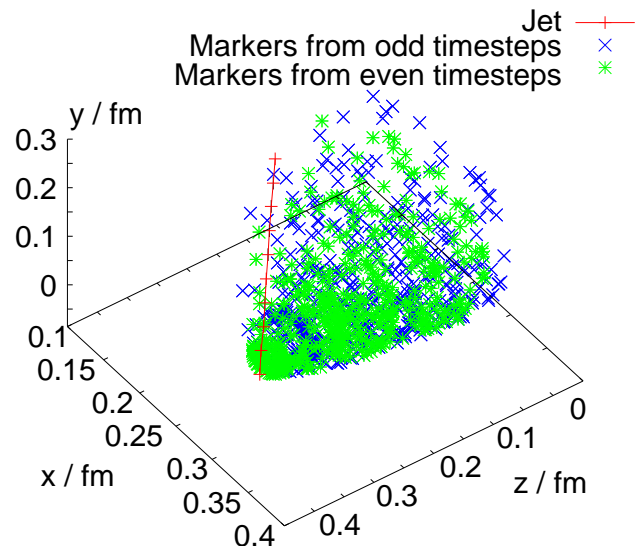


FIG. 1: (Color Online) Wave markers for a jet propagating through a peripheral RHIC-collision after 10 timesteps. The jet was started near the center of the collision with a rapidity of  $y = 1.1$ . The red line shows the trajectory of the jet, the blue crosses and green stars show the wave markers started at odd and even timesteps, respectively.

Since the underlying hydro-evolution is calculated using an EoS with a constant speed of sound (see Eq. (10)), it would be inconsistent to use a density-dependent speed of sound for the propagation of the sound waves. Therefore, propagation always happens with  $c_s = 1/\sqrt{3}$ .

### C. Mach cones

In order to see the collective phenomenon of a Mach cone, the region occupied by wave markers is reshaped with a set of lines, so-called wave lines. They go along the surface of that region, starting at the position of the jet. A handy analogy to this are longitudes going from the pole of the earth along its surface and thereby reshaping it.

The wave lines are equally distributed azimuthally around the jet's direction. Their nodes are positions of marker particles. By restricting the possible nodes to those marker particles that are in the correct azimuthal slice the azimuthal position of the wave lines is fixed.

The sheer surface of the area might be very distorted or irregular due to numerical reasons. For instance, due to the finite density of timesteps, the surface will contain large portions of the same elementary waves (in the limit of infinitely many elementary waves each of these only contribute one point on a circle in a plane orthogonal to the jet's direction). Also, the random direction of the wave markers and their finite number may cause distortion. It might be the case that in the area where a given elementary wave should represent the surface there is no wave marker to determine a possible node.

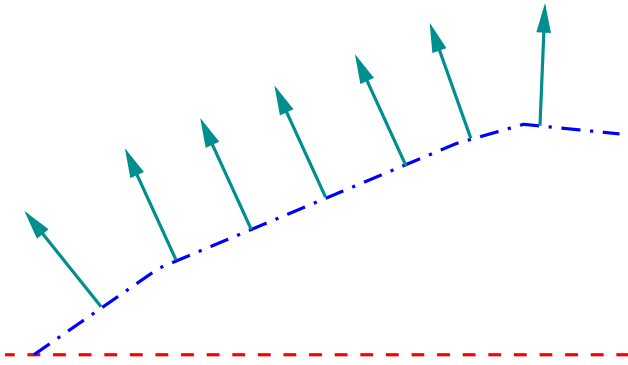


FIG. 2: (Color Online) Sketch on how the signals are created from the wave lines. The red dotted line shows the jet trajectory, the blue dash-dotted line a wave line. The arrows are perpendicular to the wave line in constant intervals along it.

In MACE, the surface is smoothed to eliminate these effects. Care is taken not to conceal physical effects during this procedure.

When all nodes are collected and the lines are complete, particle flow is considered to be orthogonal to the wave lines. The lines are now taken *as is*. To find the places on which to insert a signal we go along the wave lines, starting from the jet, and insert a signal after fixed distances. Momentum is inserted in the plane where the wave line is, orthogonal to the jet direction (see Fig. 2).

The signals are taken directly and mapped into correlation functions. There is no new velocity or momentum profile created using signal and underlying hydrodynamical fields. Therefore, background-subtracted data are obtained more easily. The correlation plots shown in section V are normalized to the number of signals.

Obviously, the position and density of wave markers is totally lost during this procedure. Instead, the density of wave lines is important. It is easy to see that this drops with the inverse of the distance to the jet axis. Since the amplitude of a Mach cone decreases with the same law, no additional, artificial decreasing of the signal has to be performed. Therefore, it is justified to keep the distance between to signals along the wave lines constant.

The region right behind the jet is treated as any other region in the model. Hence, the cones really have a sharp top. Non-linear behaviour and a rounder shape in this region is not included.

## V. RESULTS

The correlation functions obtained with different velocity fields created from different initial states show a very common shape. Both in central RHIC- (see Fig. 3) and central LHC-Collisions (see Fig. 4) ( $\sqrt{s_{NN}} = 130$  GeV and  $\sqrt{s_{NN}} = 5.5$  TeV, respectively) the averaged correlation functions show a clear double-peaked structure in the backward hemisphere. Also, in all cases those two peaks are not at the expected positions  $\Delta\varphi = \pi \pm$

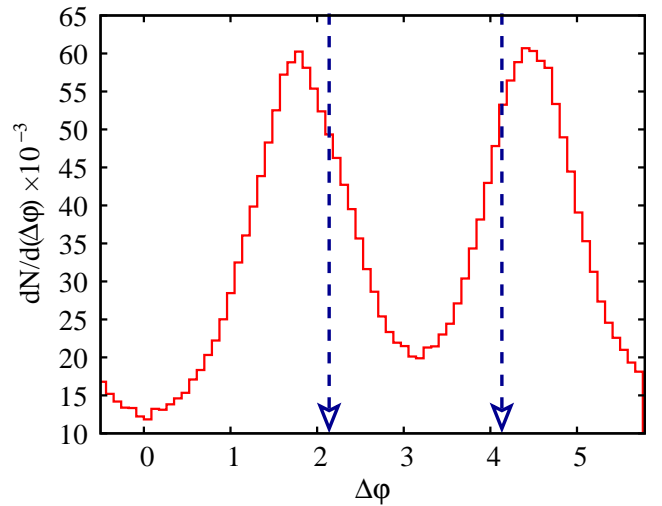


FIG. 3: (Color Online) Two-particle correlations (backward hemisphere) for central gold-on-gold RHIC-collisions ( $\sqrt{s_{NN}} = 130$  GeV and  $b = 0$ ). The plot shows the average over 1 000 arbitrary jets. The arrows show the “perfect mach positions”  $\Delta\varphi = \pi \pm \cos^{-1} c_s$ .

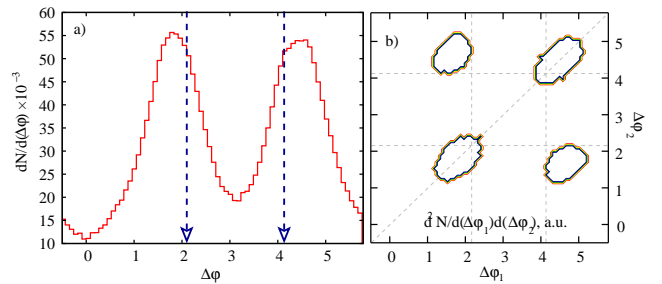


FIG. 4: (Color Online) Two- (a) and Three- (b) particle correlations (backward hemisphere) for central lead-on-lead LHC-collisions ( $\sqrt{s_{NN}} = 5.5$  TeV and  $b = 0$ ). Both plots show the average over 1 000 arbitrary jets. The arrows show the “perfect mach positions”  $\Delta\varphi = \pi \pm \cos^{-1} c_s$ .

$\cos^{-1} c_s$ , which would be  $\Delta\varphi_1 = 2.2$  and  $\Delta\varphi_2 = 4.1$ . Instead, they are systematically at positions further apart, so the angle to the backward direction is systematically bigger. The magnitude of this shift is also very constant among the considered cases; it is about  $\delta\Delta\varphi \approx 0.2$ . Correlations for mid-central RHIC collisions (not shown) do not show a significantly different picture.

Three-particle correlations (see Fig. 4 (b)) show the expected four-peaked structure, but also here it can be seen that these peaks are not at the expected position.

A trigger on the direction of the jet (see Fig. 5) gives the same picture. Both the midrapidity jets and the forward jets result in correlation functions with peaks at the same positions as the peaks from the untriggered data. Please note that since all plots are made for central collisions, in which the system is azimuthally symmetric, an additional trigger on in-/out-of-plane-jets is meaningless.

While triggering on the rapidity of a jet is experi-

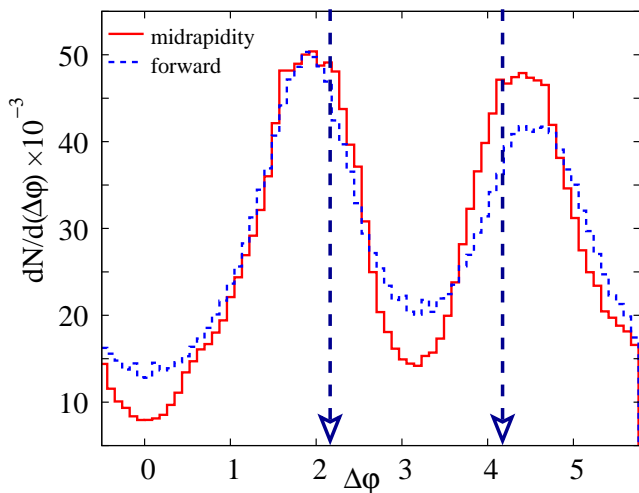


FIG. 5: (Color Online) Two-particle correlations (backward hemisphere) for central LHC-collisions for forward- and midrapidity-jets. Both lines show the average over 250 jets from arbitrary positions. The arrows show the “perfect mach positions”  $\Delta\varphi = \pi \pm \cos^{-1} c_s$ .

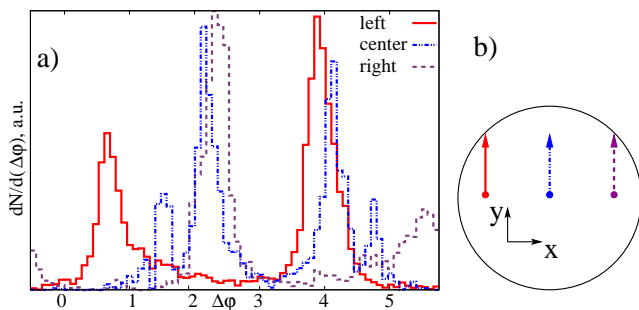


FIG. 6: (Color Online) (a): Two-particle correlations (backward hemisphere) for central LHC-collisions for single midrapidity-jets started from different positions in the collision zone. (b): The starting positions for the jets shown in (a).

mentally a very easy task, it is impossible to model-independently measure the origin of a jet inside the reaction zone. But since all data with averaged origins show the same behaviour, it is interesting to look for cases where the origin is fixed.

In Fig. 6 (a) the correlation functions for three different jet origins (which are shown in Fig. 6 (b)) are shown. All jets go in midrapidity and into the same azimuthal direction. The latter should not make any difference due to the symmetry present in central collisions.

The figure shows how much the correlation functions differ. While the correlation function from the centrally started jet is both symmetric around  $\pi$  and has the peaks at the expected positions  $\Delta\varphi \approx \pi \pm 0.96$ , the more peripherally started jets have one of the peaks much smaller than the other and far away from the expected position. When averaging over lots of jets coming from peripheral positions, it is obvious why the correlation function looks like the ones shown in Figs 3, 4 and 5.

One important result is that no correlation function shows the “wide-peak”-structure as observed at RHIC.

## VI. CONCLUSIONS

MACE shows that if sound waves are created by a jet propagating through Quark-Gluon-Plasma, two- and three-particle correlation functions will show the expected double- and fourfold-peaked structures. The cone is not washed out by collective flow.

The peaks will, though, not be at the expected “perfect mach positions”  $\Delta\varphi_{1,2} = \pi \pm \cos^{-1} c_s$ , but shifted to positions expected for lower sound velocities. This shift of the maxima is strong enough ( $\delta\Delta\varphi_{\max} \approx 0.2$ ) to feign the presence of Hadron gas in favour of the (actually present) Quark-Gluon-Plasma.

The presence of a double-peaked structure (for two-particle correlations) means that no wide-peak structure arises in MACE. That means that it is not created by an enormous shift of the conical angles by flow. Non-linear effects in the cone which might occur (spatially) near the jet may be a better explanation. If the created shape is not a true cone, but a cone with a round top, particle emission will be enhanced in backward region with respect to the results from MACE. Also, a slowing down of the jet will change the correlation signal to enhance the backward region.

Event-by-event analysis might give better insight into the real speed of sound. Correlation functions from midrapidity jets that are symmetric around  $\pi$  show their peaks at the expected positions. But single-event triggers may be useless due to event-by-event fluctuations.

## Acknowledgments

This work has been supported by the German National Academic Foundation. B. Bäuchle wishes to thank Hannah Petersen, Barbara Betz, Leonid Satarov, Marcus Bleicher and Igor Mishustin for fruitful discussions.

[1] C. Adler et al. (STAR), Phys. Rev. Lett. **90**, 082302 (2003), nucl-ex/0210033.  
 [2] J. Adams et al. (STAR), Phys. Rev. Lett. **91**, 072304 (2003), nucl-ex/0306024.

[3] F. Wang (STAR), J. Phys. **G30**, S1299 (2004), nucl-ex/0404010.  
 [4] J. Adams et al. (STAR), Phys. Rev. Lett. **95**, 152301 (2005), nucl-ex/0501016.

- [5] B. Jacak (PHENIX), J. Phys. Conf. Ser. **50**, 22 (2006), nucl-ex/0508036.
- [6] F. Wang (STAR), Nucl. Phys. **A774**, 129 (2006), nucl-ex/0510068.
- [7] N. N. Ajitanand (PHENIX), Acta Phys. Hung. **A27**, 197 (2006), nucl-ex/0511029.
- [8] F. Wang, Nucl. Phys. **A783**, 157 (2007), nucl-ex/0610011.
- [9] L. Molnar (2007), nucl-ex/0701061.
- [10] J. G. Ulery and F. Wang (2006), nucl-ex/0609017.
- [11] F. Wang, AIP Conf. Proc. **892**, 417 (2007), nucl-ex/0610027.
- [12] J. G. Ulery (STAR) (2007), arXiv:0704.0224 [nucl-ex].
- [13] S. Kniege and M. Ploskon (CERES) (0300), nucl-ex/0703008.
- [14] W. Scheid, J. Hofmann, and W. Greiner (1974), in \*Berkeley 1974, Proceedings, Lawrence Berkeley Lab Lbl- 3675\*, Berkeley 1974, 1-50.
- [15] J. Hofmann, H. Stoecker, W. Scheid, and W. Greiner (1975), report of the Workshop on BeV/nucleon Collisions of Heavy Ions: How and Why, Bear Mountain, New York, 29 Nov - 1 Dec 1974.
- [16] J. Hofmann, H. Stoecker, W. Scheid, and W. Greiner (1975), in \*Muenchen 1975, Fourteenth International Cosmic Ray Conference, Vol.7\*, Muenchen 1975, 2297-2302.
- [17] H. G. Baumgardt et al., Z. Phys. **A273**, 359 (1975).
- [18] J. Hofmann, H. Stoecker, U. W. Heinz, W. Scheid, and W. Greiner, Phys. Rev. Lett. **36**, 88 (1976).
- [19] J. Hofmann et al. (1976), in \*Dubna 1976, Proceedings, Selected Topics In Nuclear Structure, Vol.2\*, Dubna 1976, 370-385.
- [20] J. Hofmann et al. (1976), in \*Trieste 1976, Proceedings, Multiparticle Production On Nuclei At Very High Energies\*, Wien 1977, 263-283.
- [21] H. Stoecker, J. F. Hofmann, W. Scheid, and W. Greiner, Fizika **9**, 671 (1977).
- [22] H. Stoecker, J. Hofmann, J. A. Maruhn, and W. Greiner (1979), in \*Erice 1979, Proceedings, Heavy Ion Interactions At High Energies\*, 133-195.
- [23] H. Stoecker, J. Hofmann, J. A. Maruhn, and W. Greiner (1979), in \*Berkeley 1979, Proceedings, Workshop On Ultrarelativistic Nuclear Collisions\*, 355-417.
- [24] H. Stoecker et al. (1980), in \*Dresden 1980, Proceedings, Extreme States In Nuclear Systems, Vol. 2\*, 23-59.
- [25] H. Stoecker, J. A. Maruhn, and W. Greiner, Phys. Rev. Lett. **44**, 725 (1980).
- [26] H. Stoecker, Nucl. Phys. **A750**, 121 (2005), nucl-th/0406018.
- [27] J. Casalderrey-Solana, E. V. Shuryak, and D. Teaney, J. Phys. Conf. Ser. **27**, 22 (2005), hep-ph/0411315.
- [28] A. K. Chaudhuri and U. Heinz, Phys. Rev. Lett. **97**, 062301 (2006), nucl-th/0503028.
- [29] L. M. Satarov, H. Stoecker, and I. N. Mishustin, Phys. Lett. **B627**, 64 (2005), hep-ph/0505245.
- [30] F. Antinori and E. V. Shuryak, J. Phys. **G31**, L19 (2005), nucl-th/0507046.
- [31] T. Renk and J. Ruppert, Phys. Rev. **C72**, 044901 (2005), hep-ph/0507075.
- [32] T. Renk and J. Ruppert, Phys. Rev. **C73**, 011901 (2006), hep-ph/0509036.
- [33] T. Renk, Acta Phys. Hung. **A27**, 263 (2006), hep-ph/0510188.
- [34] J. Casalderrey-Solana and E. V. Shuryak (2005), hep-ph/0511263.
- [35] T. Renk and J. Ruppert, Phys. Lett. **B646**, 19 (2007), hep-ph/0605330.
- [36] T. Renk, Eur. Phys. J. **C49**, 13 (2007), hep-ph/0607035.
- [37] T. Renk (2006), hep-ph/0608333.
- [38] E. Shuryak, Nucl. Phys. **A783**, 31 (2007), nucl-th/0609013.
- [39] A. K. Chaudhuri, Phys. Rev. **C75**, 057902 (2007), nucl-th/0610121.
- [40] E. Shuryak, Nucl. Phys. **A783**, 39 (2007).
- [41] T. Renk and K. J. Eskola (2007), hep-ph/0701097.
- [42] J. Casalderrey-Solana (2007), hep-ph/0701257.
- [43] T. Renk and J. Ruppert (2007), hep-ph/0702102.
- [44] H. Stoecker, B. Betz, and P. Rau, PoS **CPD2006**, 029 (2006), nucl-th/0703054.
- [45] A. K. Chaudhuri (2007), arXiv:0705.1059 [nucl-th].
- [46] A. K. Chaudhuri (2007), arXiv:0706.3958 [nucl-th].
- [47] A. A. Amsden and F. H. Harlow, J. Comp. Phys **3**, 94 (1968).
- [48] F. H. H. A. A. Amsden, A. S. Goldhaber and J. R. Nix, Phys. Rev. **C17**, 2080 (1978).
- [49] R. B. Clare and D. Strottman, Phys. Rept. **141**, 177 (1986).
- [50] D. Strottman, Lecture Notes in Mathematics **1385**, 278 (1989).
- [51] N. S. Amelin et al., Phys. Lett. **B261**, 352 (1991).
- [52] V. K. Magas, L. P. Csernai, and D. D. Strottman, Phys. Rev. **C64**, 014901 (2001), hep-ph/0010307.
- [53] V. K. Magas, L. P. Csernai, and D. Strottman, Nucl. Phys. **A712**, 167 (2002), hep-ph/0202085.